

Journal of
Mechanics of
Materials and Structures

**A MULTILEVEL NUMERICAL MODEL QUANTIFYING CELL
DEFORMATION IN ENCAPSULATED ALGINATE STRUCTURES**

Kalyani Nair, Karen Chang Yan and Wei Sun

Volume 2, N° 6

June 2007



mathematical sciences publishers

A MULTILEVEL NUMERICAL MODEL QUANTIFYING CELL DEFORMATION IN ENCAPSULATED ALGINATE STRUCTURES

KALYANI NAIR, KAREN CHANG YAN AND WEI SUN

Mechanical forces not only deform cells, but also alter their functions due to biological responses. While current biomanufacturing processes are capable of producing tissue scaffolds with cells encapsulated, it is essential to understand cell responses to process-induced mechanical disturbances. In this study the stresses and deformations of encapsulated cells under compressive loads are quantified via a multilevel nonlinear finite element approach. The macrolevel model is used to mechanically characterize the alginate-cell construct. At the microlevel, the effects of alginate concentration, cell model, and the microlevel geometric heterogeneity on cell deformation are examined. Cells are modeled as single phase inclusions containing only a nucleus phase; then as a two-phase inclusion comprised of a nucleus phase and cytoplasm phase. This study also analyzes the effects of two geometrical parameters—namely, cell size and cell distribution—on the local stress levels of the cell. Subsequent statistical analyses provide insight into the degree of influence of these factors. The study shows that cells embedded in a higher alginate concentration, 3% w/v, experience higher stress levels as compared to cells embedded in a lower alginate concentration, 1.5% w/v. Furthermore, analysis of the geometric heterogeneity indicates that there is a much higher stress concentration in areas where cells are clustered together as compared to areas where cells are relatively isolated.

1. Introduction

Tissue engineering is a multidisciplinary field involved in creating functional 3D tissues using cells along with scaffolds that facilitate cell growth, organization and differentiation [Griffith and Swartz 2006]. Cell functions are affected by a multitude of cues arising from the extracellular matrix (ECM) components, mechanical perturbations, surface chemistry, chemical and biological signals from neighboring cells. Studies have shown that mechanical forces are essential to living cells, especially for the bone and endothelium cells that are subjected to specific forces as a part of the native physiological environment [Bao and Suresh 2003]. Mechanical forces not only deform cells, but also induce biological responses, and result in altered functions [Ingber 1997; Breuls et al. 2002]. Furthermore, with the advent of biofabrication technology, tissue scaffolds can be fabricated with cell seeded and/or encapsulated. Experimental studies have demonstrated that the mechanical disturbance due to the fabrication processing affects cell viability in the formed scaffold construct [Khalil 2006]. In this connection, understanding the underlying mechanisms and developing mathematical models to predict cell behavior in a designed surrounding would aid in maintaining and controlling the phenotype of the cells to form functional tissue in an engineered construct.

Keywords: scaffold, tissue engineering, multilevel, computational, cell.
The authors acknowledge support from US NSF Grant No. 0427216.

Recently, there have been increasing efforts to study the effects of the microenvironment on cell morphology and function, both experimentally and numerically. Pelham and Wang [1997] investigated the cell responses to the stiffness of the substrates. NRK epithelial cells and 3T3 fibroblasts were cultured on the substrates with variable physical properties, but a controlled chemical environment. Both NRK epithelial cells and 3T3 fibroblasts were well spread and looked similar to cells cultured on glass or plastic substrates; NRK cells became less well spread and irregularly shaped when more flexible substrates were used.

Guilak and Mow [2000] developed a multilevel biphasic finite element model of the chondrocyte within an explant of cartilage to characterize and predict the biomechanical interactions between the chondrocyte and the extracellular matrix as well as determine the influence of cell and tissue properties on the local stress-strain environment. They assumed that cells do not contribute to the mechanical properties of the tissue and considered a single chondrocyte under unconfined compression. Breuls et al. [2002] have introduced a large-strain model based on a multilevel finite element approach that predicts the local cell deformations in engineered tissue constructs, subjected to macroscopic external loads. Although numerical analyses have demonstrated the presence of microlevel physical and geometrical heterogeneity in terms of the cell stress and deformation, the degree of effects as well as the dominance among various parameters remains unanswered. Caille et al. [2002] found that the nucleus and the cytoplasm have considerable differences in terms of material properties, which may not be negligible, especially at the microlevel. Furthermore, the effects of material stiffness on cells are critical when fabricating scaffolds for tissue engineering applications making it of great interest as well.

The objective of this study is to characterize the mechanical behavior of alginate tissue constructs in the macroscale and to quantify the local stresses and deformations at a cellular level when the tissue construct is subjected to macrolevel loads. Moreover, this study quantifies the effects of microlevel physical and geometrical heterogeneity on cell deformation. Specifically, it examines the effects of the cell substructure, the matrix material stiffness, and the cell geometric distribution in terms of location and size. Here we consider alginate as the matrix material owing to its excellent biocompatibility [Drury et al. 2004] and capability to fabricate three dimensional scaffolds [Khalil et al. 2005].

In conjunction with our initial experimental studies on alginate constructs with encapsulated endothelial cells, the present study also focuses on endothelial cells. Endothelial cells are usually present as linings in the entire circulatory system and are subjected to several different types of mechanical stimuli including hydrostatic pressure, fluid shear stress, and deformation [Cines et al. 1998]. The strain magnitudes in the aorta and large arteries range between 2%–10% [Dobrin 1978; Wedding et al. 2002]. Wille et al. [2004] have studied the effects of cyclic stretching as well as compression at strain rates of 2%–10% on the morphological responses of endothelial cells. This analysis is carried out to investigate the local stress/deformation of the cells when subjected to compression at the physiological level and beyond.

The analyses are conducted via a multilevel nonlinear finite element method. The macrolevel analysis is a nonlinear finite element model that characterizes the macroscopic behavior of alginate discs with encapsulated endothelial cells under load. The analysis simulates a compression test on the constructs and focuses on characterizing its mechanical properties. This, however, does not provide any insight of the stresses and deformations occurring at the cellular levels. Upon the results of the macroanalysis, a microlevel analysis is conducted to determine local stress/strain fields in a selected region with the

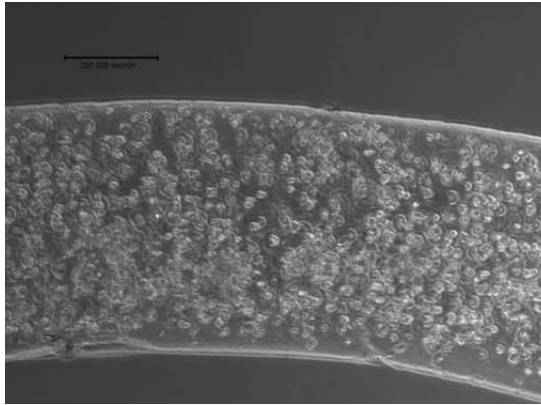


Figure 1. Fluorescent live/dead image of alginate construct with encapsulated rat heart endothelial cells.

encapsulated cells. Numerical results are determined and analyzed to quantify the effects from various sources on the local cell responses.

The paper is organized as follows. Section 2 describes the multilevel finite element approach that is applied in this study. Section 3 details the numerical procedure and model development, which includes the macrolevel and microscale analysis in Sections 3.1 and 3.2, respectively. In addition to the material model and cell model, three microfinite element models are developed to incorporate the geometrical heterogeneity, namely, encapsulated cells with random location and size, with random location and uniform size, and with uniform location and size. The latter two cases are presented for comparative purposes. The details of the results along with the discussions are given in Section 4.

2. Framework for analysis of cell encapsulated constructs: multilevel finite element approach

Alginate-based tissue scaffolds are fabricated using a proprietary multinozzle biopolymer deposition system [Khalil et al. 2005; Khalil 2006]. Upon examining the alginate scaffold with encapsulated endothelial cells, the size of cells is very small compared to the dimensions of the macrostructure (see Figure 1), therefore, multilevel analysis is necessary, especially for determining the cell responses. The paper focuses on the analysis of alginate-cell structures at three different scales.

At the macrolevel a nonlinear numerical model is developed to characterize the mechanical properties of the construct. For specific applications in tissue engineering it becomes necessary and indispensable to understand the stresses at the microenvironment of the encapsulated cells since cells respond to such stresses and their functions are highly dependent on such mechanical cues. Assuming statistical homogeneity, the multilevel finite element analysis may be utilized to determine the cell responses to the external load and further understand the effects of the system parameters from the different scales. A microlevel model has been developed to analyze the local effects around the cell boundaries, assuming that cells are inclusions within the alginate structure. The effects of physical and geometric heterogeneity on cells have been quantified as well. At the microlevel, the influence of substructures within the cell model contributes significantly to the stress distribution in the environment. Therefore, the study

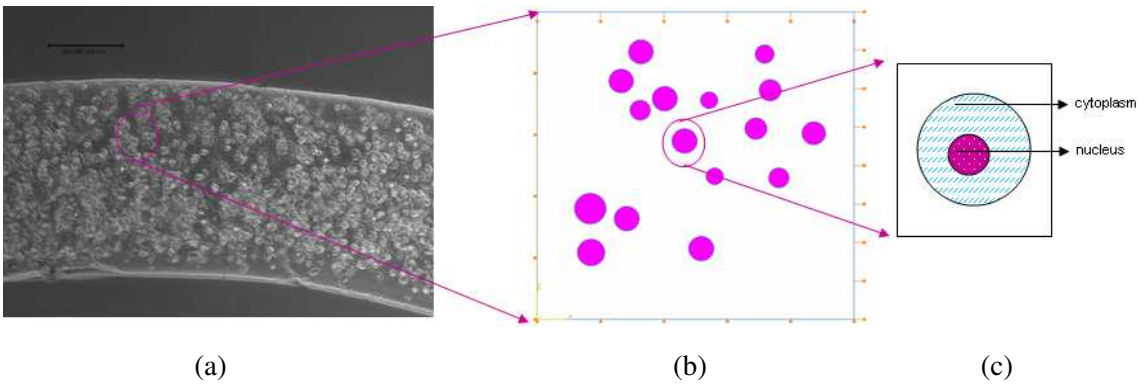


Figure 2. Multilevel approach applied to cell encapsulated alginate construct: (a) macrolevel analysis of discs under compression; (b) microlevel analysis incorporating random cell size and cell distribution; (c) analysis incorporating random cell size and cell distribution along with nucleus and cytoplasm.

attempts to analyze the microenvironment when including more specific cellular substructures such as the cytoplasm within the cell-model geometry. When analysis is conducted at the microscale, more information about cell membrane injury can be derived since the cytoplasm is less rigid than the nucleus and is prone to damage at lower levels of stress. Figure 2 indicates the multilevel approach along with the different microstructures integrated in the analysis. Experimental evidence suggests that the contribution of endothelial cells to the macroproperties is negligible

The multilevel finite element analysis has been developed and applied to link the microscopic behavior and the macroscopic phenomena of heterogeneous engineering materials [Smit et al. 1998; Kouznetsova et al. 2001; Wang and Yan 2005]. The fundamental assumption that enables this practice is statistical homogeneity. A heterogeneous body consisting of a blend of two materials, in general, possesses randomly distributed properties. For a complete description of the physical properties, each property is a random spatial function, and all of their joint probability distributions must be known. For instance, the microstructure can be described by the n -point phase probability function S_n , which is the probability of finding n points simultaneously in phase 1 [Quintanilla and Torquato 1997] defined by

$$S_n(x_1, x_2, \dots, x_n) = \left\langle \prod_{i=1}^n I(x_i) \right\rangle, \quad I(x) = \begin{cases} 1, & x \text{ in phase 1,} \\ 0, & \text{otherwise,} \end{cases}$$

where $I(x)$ is the indicator function of phase 1, and the angular brackets denote an ensemble average over the possible realizations of the material. For statistical homogeneous media one can equate the ensemble averages with volume averages in the infinite volume limit, that is, ergodicity [Torquato 1998]. In practice a representative volume element (RVE) needs to be selected to represent the material adequately, to ensure, in particular, the one-to-one correspondence between the macro and microlevels. For a statistically homogeneous material under load, the local macroscopic deformation and stresses are equal to the averaged deformation and stresses of the RVE as given in equations below [Smit et al. 1998]. The deformation tensor $F(y_0)$ refers to the initially undeformed configuration at reference position y_0 ,

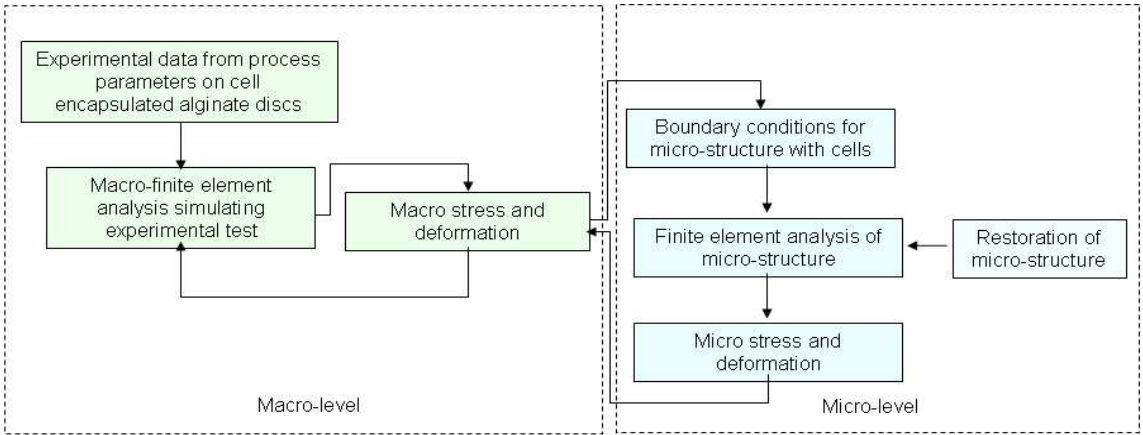


Figure 3. Flow chart of the multilevel finite element analysis procedure.

and the volume averaging is performed over the initial volume of the unit cell V_0 .

$$F_{\text{macro}} = \bar{F}_{\text{RVE}} = \frac{1}{V_{0\text{RVE}}} \int_{y_0 \in V_{0\text{RVE}}} F(y_0) dV_0, \quad \sigma_{\text{macro}} = \bar{\sigma}_{\text{RVE}} = \frac{1}{V_{\text{RVE}}} \int_{y \in V_{\text{RVE}}} \sigma(y) dV.$$

F_{macro} and \bar{F}_{RVE} are the macro and the RVE-averaged deformation gradient tensors, respectively, and σ_{macro} and $\bar{\sigma}_{\text{RVE}}$ are the macro and the RVE-averaged stress tensor, respectively. The average stress in the RVE $\bar{\sigma}_{\text{RVE}}$ is the volume-averaged Cauchy stress tensor, where $\sigma(y)$ represents the stress tensor at position y . The averaging occurs over the current volume of the RVE because the Cauchy stress is defined in the current deformed configuration [Smit et al. 1998]. F_{macro} and σ_{macro} can be related through the material constitutive relation. In case of hyperelastic material [ABAQUS 2002], the material constitutive relation can be expressed as

$$\delta W = \int_{V_0} \det(F_{\text{macro}}) \sigma_{\text{macro}} : \delta D(F_{\text{macro}}) dV_0 = \int_{V_0} \delta U(F_{\text{macro}}) dV_0,$$

where δW is the variation of work, and δU is the variation of strain energy.

Figure 3 is a schematic of the multilevel modeling approach applied in this study. Initial experiments are conducted to characterize the overall/macro properties of the system under compressive load, and corresponding macrofinite element analyses are carried out to validate the experimental results and provide the macrodeformation and stresses. Detailed microstructures are restored to a region of interest, and microlevel analyses are then performed to determine the local deformation and stresses within the region.

3. Numerical procedure: macro and microlevel characterization of alginate-cell constructs

A nonlinear macrolevel numerical model has been developed to analyze the structural properties of three dimensional tissue engineering scaffolds. The model is also validated experimentally. Details of the

procedure are explained in Section 3.1. A nonlinear microlevel analysis is then conducted to capture the stress and deformation of the encapsulated cells in the scaffold when subjected to external compression. The physical and geometrical heterogeneity is modeled to analyze the degree of influence of these effects on the cell's microenvironment. Section 3.2 describes the microlevel modeling procedure in detail.

3.1. *Macrolevel analysis characterizing mechanical properties of cell encapsulated alginate discs.*

Uniaxial compression tests are performed to measure the mechanical properties of alginate (Manugel) using a 4442 Instron mechanical tester. Gel samples are prepared in a cell culture 24-wellplate. Rat heart endothelial cells (500,000 cells/ml) are encapsulated in 1.5% w/v alginate concentration and are cross linked with 0.5% calcium chloride to form 2.1 mm thick 4.5 mm radii alginate discs. Six specimens are tested and a maximum compressive strain of up to 40% is applied to obtain the stress-strain curve as shown in Figure 4b. Previous experiments indicate that the stiffness of the alginate increases as the concentration increases, especially over the range of 1%–3% w/v [Khalil 2006].

Axisymmetric finite element models are developed simulating the virtual compression tests based on the experimental specimen geometry. With the obtained experimental data, the Marquardt Levenberg nonlinear least square optimization (MLNLS) algorithm is used to fit the experimental data with the neoHookean, Mooney–Rivlin and Ogden models. The three models have been used for comparative purposes to determine the most accurate material model that can best fit the experimental data. The constants are obtained by using the MLNLS optimization algorithm. The algorithm minimizes the error E between the experimental stress, T_{exp} , and the nominal stress, T_i , calculated from the strain energy polynomial [ABAQUS 2002], for each material model

$$E = \sum_{i=1}^n \left(1 - \frac{T_i}{T_{\text{exp}}} \right)^2, \quad T_i = \sum_{i=1}^N \frac{2\mu}{\alpha} (\lambda u^{\alpha-1} - \lambda u^{-0.5\alpha-1}).$$

Between the three models considered, the neoHookean model incorporates only a single material constant and has the simplest formulation for the strain energy density function. The Mooney–Rivlin model is capable of taking into account the deviations arising from other Gaussian and neoHookean models [Boyce 2000]. In these two models the strain energy density function is expressed in terms of the stretch variants. In the Ogden model [Boyce 2000; ABAQUS 2002], the strain energy is expressed in terms of the principal stretches ($\lambda_i = 1, 2, 3$) as

$$W_o = \sum_{i=1}^n \frac{2\mu_i}{\alpha_i^2} (\lambda_1^{-\alpha_i} + \lambda_2^{-\alpha_i} + \lambda_3^{-\alpha_i} - 3).$$

Here the hyperelastic Ogden material model is used for the alginate disc with embedded endothelial cells since it produces a much closer approximation to the test data of the nonlinear hydrogel than the other strain energy density functions. Here, μ_i and α_i are material-dependent constants, and n is the degree of summation, which can be varied to best fit the data at hand allowing additional flexibility. In the present study the Ogden polynomial with $n = 4$ is used for an alginate concentration of 1.5% w/v, and $n = 3$ for 3% w/v.

Although physical meanings associated with the constants are often not clear in phenomenological models, the Ogden material constants can be related to the shear modulus as $G = \sum_{i=1}^N \mu_i$ [ABAQUS 2002].

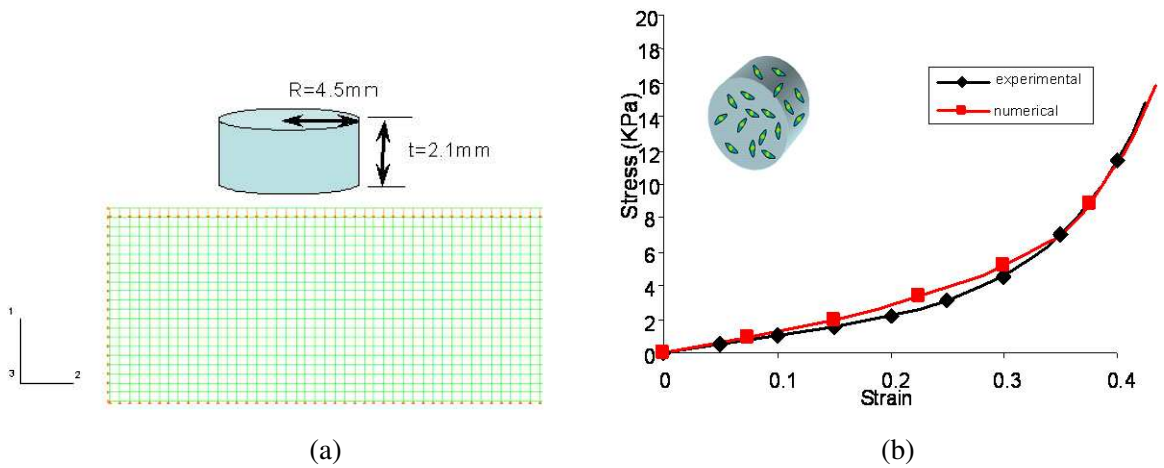


Figure 4. Macrolevel characterization of encapsulated bulk alginate discs: (a) axisymmetric FE model with loading and boundary conditions; (b) validation of numerical model with experimental data (nominal stress-strain).

The loading and boundary conditions are applied to simulate the experimental compression test, and the stress-strain curve is plotted to match up with the experimental curve. Figure 4(a) illustrates the macrolevel finite element model along with the loading and boundary conditions. Symmetric boundary conditions are applied along the vertical axis of symmetry, and uniform displacement is applied on the top surface of the sample to simulate the experimental compression test. After running the analysis for 40% strain, the nominal stress-strain curve is plotted and compared with the experimental measurements as shown in Figure 4(b). In addition, it is assumed that alginate does not exhibit any viscoelastic properties because the model predicts the mechanical properties of the scaffold at the instant it has been fabricated.

3.2. Microlevel analysis: effects of physical and geometrical variations on local cell environment.

Microlevel numerical models are developed to determine the microstress and deformation fields and the effects of microenvironment on cell responses. Ideally, the microlevel analysis should be done with realistic 3D representation of the microstructure. However, the computation of such a model involving enormous number of degree of freedom is extremely demanding, hence two-dimensional approximations are often used to circumvent the difficulty [Smit et al. 1999]. In the present study, a two-dimensional simplification (axisymmetry) is utilized. This particular simplification can be justified with two assumptions. First, we assume that the presence of cells does not influence the overall mechanical properties of the scaffold. Secondly, the cells are randomly distributed in the cylindrical specimen. Now consider any given vertical plane cutting through the center of the specimen. From the latter, the circular intersections of the cells and the cutting plane are randomly distributed on the resulting cross section in terms of location and size. Hence a 2D model with a random distribution of cells modeled as inclusions is considered as an approximated representation of a given cross section.

The loading and boundary conditions are extracted from the macrolevel analyses of the alginate specimen with 20% and 30% compression. Although such strain magnitudes are beyond the physiological levels (for instance, for the aorta and large arteries one has 2%–10% [Dobrin 1978; Wedding et al. 2002]),

they may be induced by fabrication process. The study includes such conditions to understand the effects of large strain on the cell, which may provide information with respect to cell damage. For adequate representation of the alginate disc with encapsulated endothelial cells, a region of $400\ \mu\text{m} \times 400\ \mu\text{m}$ is selected; based on the cell volume fraction, sixteen cells are included. Two alginate concentrations, 1.5% w/v and 3% w/v, are considered due to the stiffness variation. Again, the Ogden material model is used to accurately capture the nonlinearity of the alginate.

The endothelial cells are treated first as single-phase inclusions, and then as two-phase inclusions. While the former simplifies the cell as a nucleus, the latter captures the contributions from both the nucleus and cytoplasm. The neoHookean material model is adopted for the nucleus, as well as the cytoplasm [Breuls et al. 2002; Caille et al. 2002; Haider et al. 2006]. The strain energy function for the neoHookean model [ABAQUS 2002] is given by $W_{NH} = a_1(I_1 - 3)$, where a_1 is a material parameter and I_1 is the first stretch invariant. The constant a_1 can be derived from the elastic modulus and Poisson's ratio as

$$a_{1\ \text{nucleus}} = \frac{4(1 + \nu_{\text{nucleus}})}{E_{\text{nucleus}}}, \quad a_{1\ \text{cytoplasm}} = \frac{4(1 + \nu_{\text{cytoplasm}})}{E_{\text{cytoplasm}}}. \quad (1)$$

Here, the elastic moduli E of the nucleus and the cytoplasm are assumed to take the value of $4462\ \text{N/m}^2$ and $323\ \text{N/m}^2$, respectively, and Poisson's ratio is 0.5 since the material is assumed to be incompressible [Caille et al. 2002]. Note that the cytoplasm is at least ten times less stiff than the nucleus. Modeling the cytoplasm and nucleus separately gives us additional information regarding damage to the cells since the cytoplasm could withstand much lower stress levels or deformations compared to the nucleus.

It is generally believed that the geometric heterogeneity at the microlevel leads to additional nonuniformity of the local stress/deformation fields; hence, it is necessary to address this for the microstructure restoration. In the present study, it is of interest to quantify this effect; therefore, three different microstructures are identified. Corresponding micro FE models are generated and analyzed, and the results so rendered are compared. Considering a realistic representation of alginate specimen with encapsulated cells, it can be observed from the microscopic image that the endothelial cells are randomly distributed with varying size. In the first assumption, the randomness in both location and size are represented and are characterized via a stochastic mean. Specifically, the random location is generated based on the equal probability and overlap constraints, while the radius is calculated using a normal distribution with a mean value $\mu = 15$ and a standard deviation $\sigma = 3$. The probability density function at position x is given by

$$f(x) = \frac{1}{\sqrt{2\pi\sigma^2}} \exp\left[-\frac{(x - \mu)^2}{2\sigma^2}\right].$$

The average diameter of endothelial cells has been reported to be in the range of 20–30 μm [Bain 2001]. The location of the cells within the microstructure is calculated by generating a uniformly distributed pseudorandom number, lying in the specified range of 0.05 to 0.035 microns. The probability density function for a continuous uniform distribution on the interval $[a, b]$ is given by

$$f(x) = \begin{cases} \frac{1}{b - a}, & a \leq x \leq b, \\ 0, & \text{otherwise.} \end{cases}$$

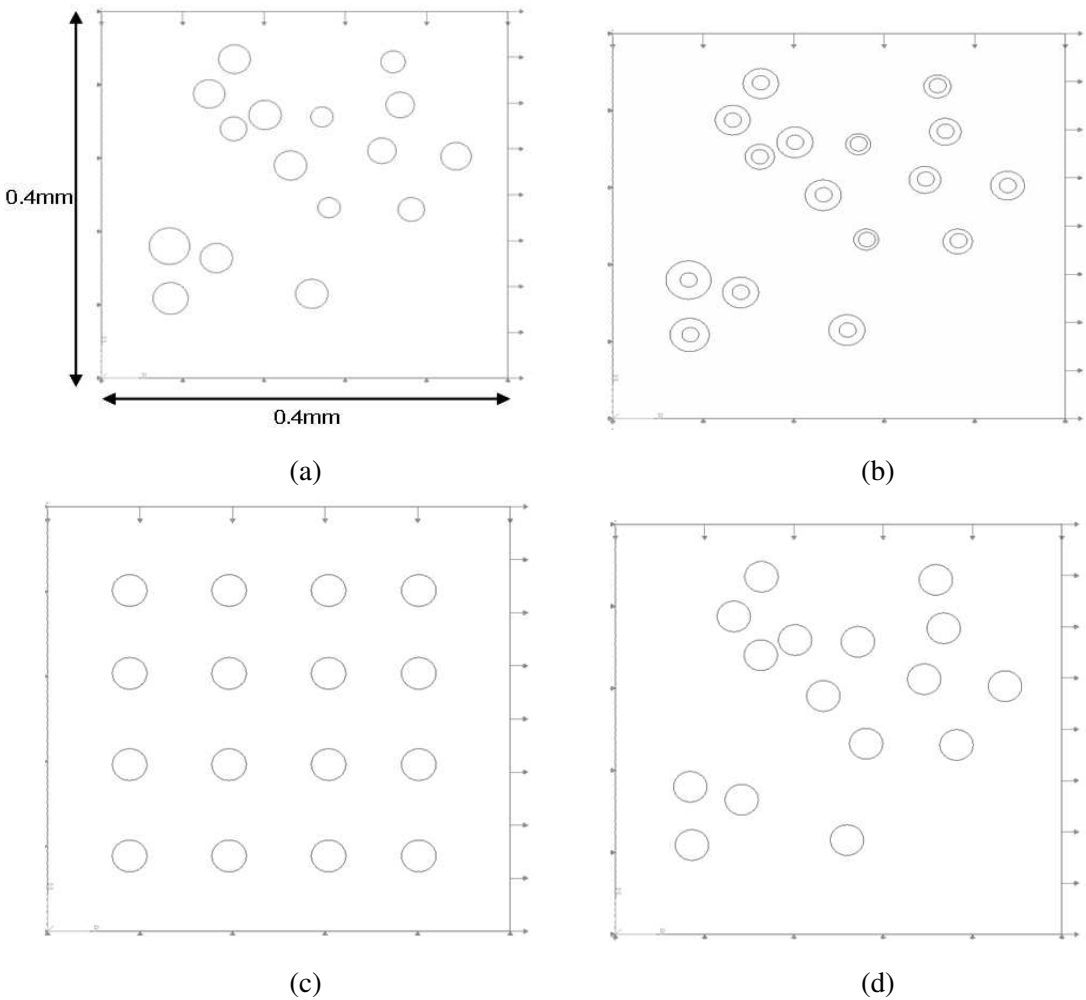


Figure 5. Microlevel analysis: (a) random cell size and cell distribution; (b) random cell size and cell distribution along with cytoplasm; (c) uniform cell size and cell distribution; (d) uniform cell size and random cell distribution.

A subset of a random set can be identified via $\sqrt{(x_i - x_k)^2 + (y_i - y_k)^2} \geq (r_i + r_k)$. Here, (x_i, y_i) is the location of any given cell, and r_i is the radius; (x_k, y_k) are the location of the cells that are adjacent to the cell i , and r_k is the corresponding radius. This is computed using a commercial mathematic tool (Mathematica ver5.2). The approach allows for closely characterizing the heterogeneity of the microstructure, especially for the cases where the cells form clusters during fabrication. Figure 5 illustrates the restored microstructure with random characteristics along with the loading of the microstructure under analysis.

The geometrical heterogeneity within the microstructure has been carried out by formulating models with varying cell size and distribution. The first model involves a geometry including uniform cell location and uniform cell size; see Figure 5c. The next model assumes a geometry incorporating random location of the cells while assuming constant cell radii; see Figure 5d. Note that both random location

and random size are considered for the microlevel model with the cell modeled as two-phase inclusions with the cytoplasm and the nucleus, see Figures 5a and 5b. The size ratio between the nucleus and the cytoplasm is assumed to be constant.

4. Results and discussion

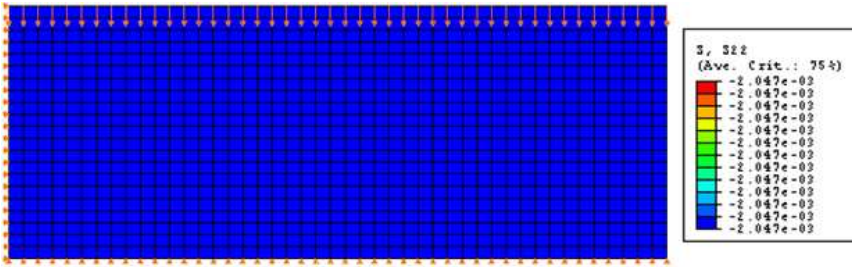
In the present study, a macrolevel model is developed to characterize the mechanical properties of alginate-cell constructs based on experimental data. A microlevel model is also developed based on information derived from the macrolevel model, and the stresses and deformations at the local cellular level are analyzed as well. Moreover, the microlevel analysis also quantifies how the stiffness of matrix material, the microstructure of the cell, and the geometric heterogeneity at the microlevel affect the local stress and deformation in the cell's microenvironment. This information leads to a better understanding of the cell responses to the mechanical force induced by the environment and a better mathematical model to predict cell viability, as well as cell damage.

Figures 6a and 6b indicate the macrolevel and the microlevel stress contours, respectively, when a 20% compressive strain is applied. As seen in Figure 6a, the macrolevel model shows uniform stress distribution and does not provide any information about the local stresses experienced by the cells. For applications in tissue engineering, it is imperative to understand the local stress levels at the cellular level since cell response to these stresses could lead to altered functions.

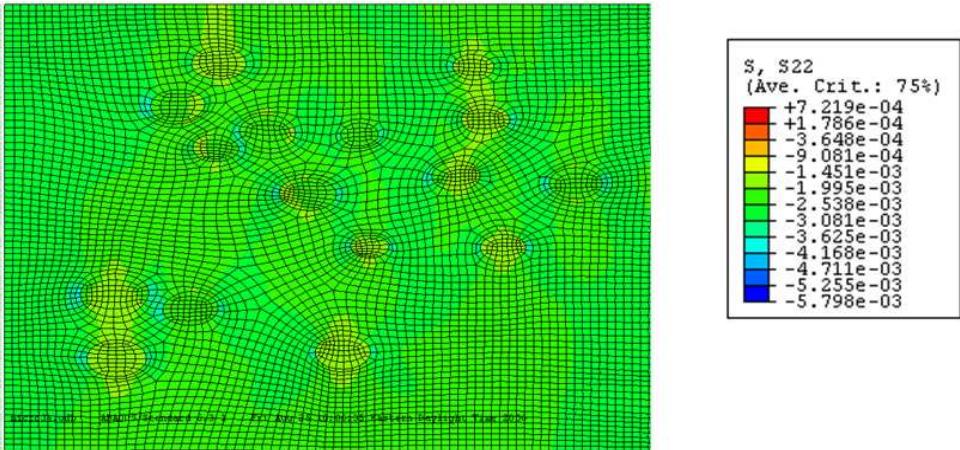
Figure 6b shows the stress contours at the cellular level wherein cells have been modeled as inclusions with the material properties assumed to be that of the nucleus. This analysis gives details regarding the microlevel stress distribution around the cells. To derive more information at this level, it is necessary to incorporate more substructures within the cell model. Figure 6c demonstrates the stress contours of the microlevel analysis where the microstructure incorporates the cell nucleus and the cytoplasm. At this level, the geometry, the density (the number of cells per unit area) and the material properties of the cell all contribute to the overall stress distribution. This analysis provides useful information about the stresses experienced by the cells in a random distribution.

4.1. Effects of matrix stiffness on cell deformation and local stress distribution. In order to study the effect of stiffness of the matrix material, alginate concentrations of 1.5% w/v and 3% w/v are considered. The stress contour plots rendered from the multilevel analysis are shown in Figure 7. The alginate gel with 1.5% w/v concentration is less stiff compared to the 3% w/v concentration. Therefore, less stress concentrations due to stiffness mismatch between the cell and matrix are introduced. We additionally observe that stresses are higher in areas where there are more cells compared to areas where the cells are isolated. The corresponding logarithmic strain contours from the analyses are given in Figure 8.

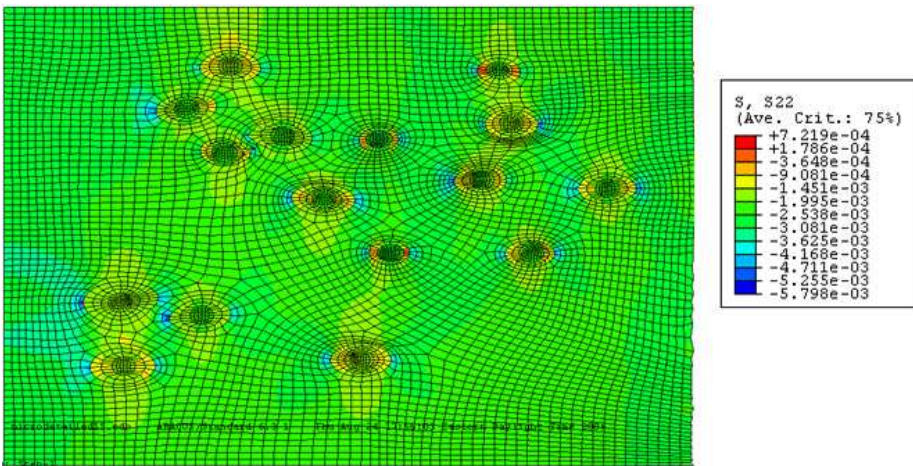
To further quantify the effect, nodal stress S_{22} along the cell boundary (90° from the horizontal direction) is considered for statistical analysis. A set of sample data for S_{22} is generated, and fitted to a normal distribution. Figure 9 plots the probability density function of S_{22} on the cell boundary for the alginate concentrations of 1.5% w/v and 3% w/v. The shift in the curves clearly indicates the difference in terms of the mean stress value. Moreover, the mean value for the stresses is about 20% higher for alginate of 3% w/v concentration than that of 1.5% w/v. Though this quantifies the stress and deformation of the cells in the different environments, this paper does not attempt to explain how these stresses or deformations affect the functionality of the cell concerned.



(a)



(b)



(c)

Figure 6. Stress (in MPa) contours for cell encapsulated alginate under 20% compressive strain: (a) macromodel for bulk discs; (b) microlevel model with cells; (c) microlevel model with cytoplasm and nucleus.

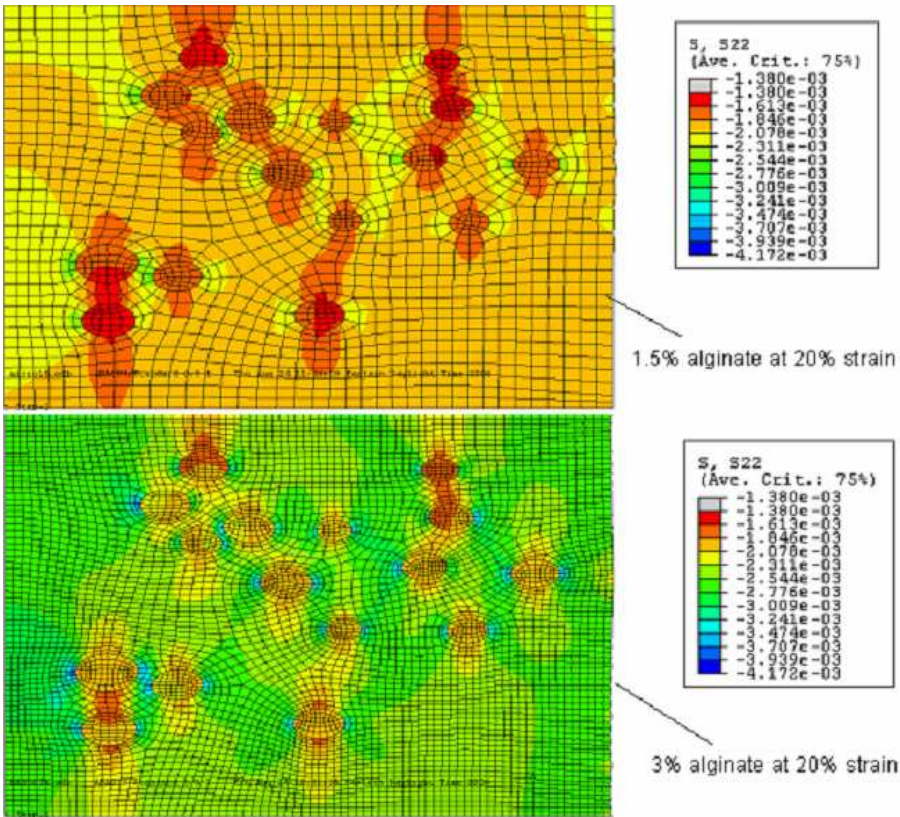


Figure 7. Stress (in MPa) contour plots for cells embedded in 1.5% w/v and 3% w/v alginate concentrations.

4.2. Effects of incorporating cytoplasm within the cell model on the local cell environment. The second factor the analysis takes into consideration is the significance of incorporating the nucleus and the cytoplasm within the cell model. It is known from literature that the material properties of the nucleus and cytoplasm are significantly different. For instance, the nucleus is about ten times stiffer than the cytoplasm [Caille et al. 2002]. Figure 10 shows a large degree of strain difference in the logarithmic strain contours between the two cases. Statistical analyses are conducted for both the stress and strain components, and the corresponding probability density function plots are shown in Figures 11 and 12, respectively. Figure 11 shows that the bell curve for the model with the nucleus and the cytoplasm has a larger standard deviation, but similar mean stress compared with the model that does not include the cytoplasm. The large deviation is due to the three phases of varying material stiffness. One can see from Figure 12 that the strains are significantly different in both cases. The shift in the curves indicates the difference in the mean strain in both cases. The model with the nucleus and cytoplasm has a higher value for the mean strain and a larger standard deviation compared with the case of only the nucleus. This can be attributed to the high degree of material property mismatch among the three regions: cell nucleus,

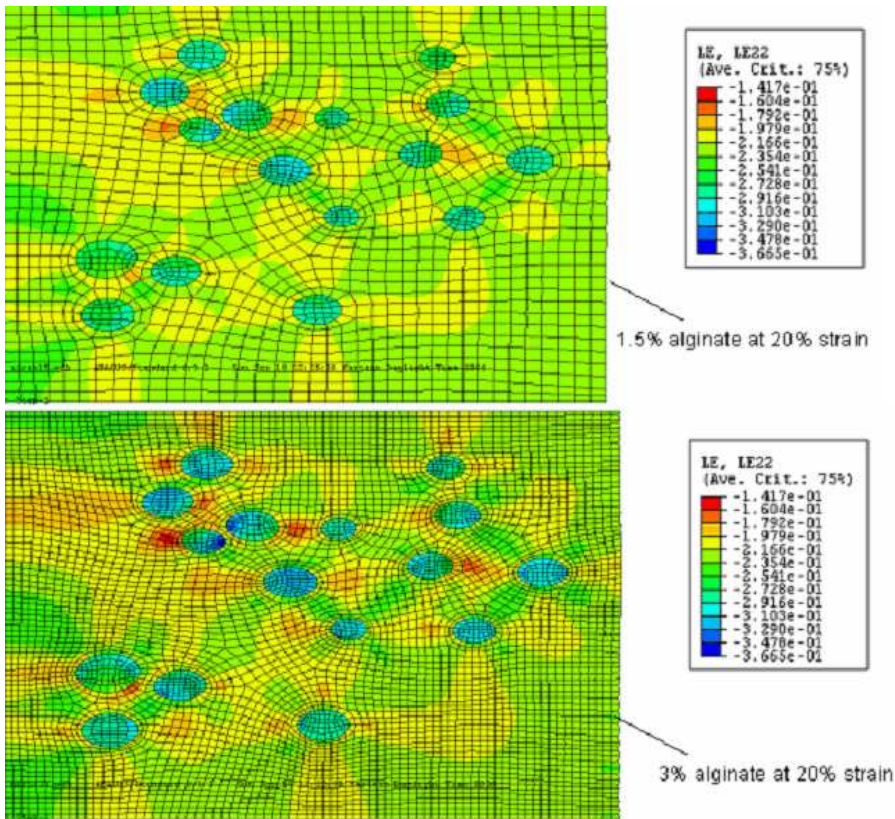


Figure 8. Logarithmic strain contour plots for cells embedded in 1.5% w/v and 3% w/v alginate concentration.

cytoplasm and surrounding alginate. Clearly analysis of the cell model incorporating the nucleus and cytoplasm provides more information that is critical to cell viability and cell function.

4.3. Effects of cell size and position on the stress distributions at the cellular level. The present study also looked into the effects of geometrical parameters, such as distributions in cell size and cell location, on the local stress at the cellular level. Specifically, the analysis aims to understand whether cell size and cell distributions in the construct adversely affect the local stresses and deformations in the cell’s surroundings. Figure 13 shows the stress contours of the three cases where the variations have been made in parameters pertaining to cell geometry and cell distribution. The stress concentrations are significantly different between the model with uniform radius and distribution and that with random cell radii and distribution. Additionally, there is a small effect on cell sizes in the analysis. Regarding cell-cell interaction, there is much higher stress concentration in areas where cells are clustered together compared to the areas where cells are relatively isolated.

Three probability density function plots of S_{22} are shown in Figure 14 for models with uniform cell size and cell distribution, with uniform cell size and random cell distribution, and with random cell size and cell distribution. The difference is clear between the model with uniform cell size/cell distribution

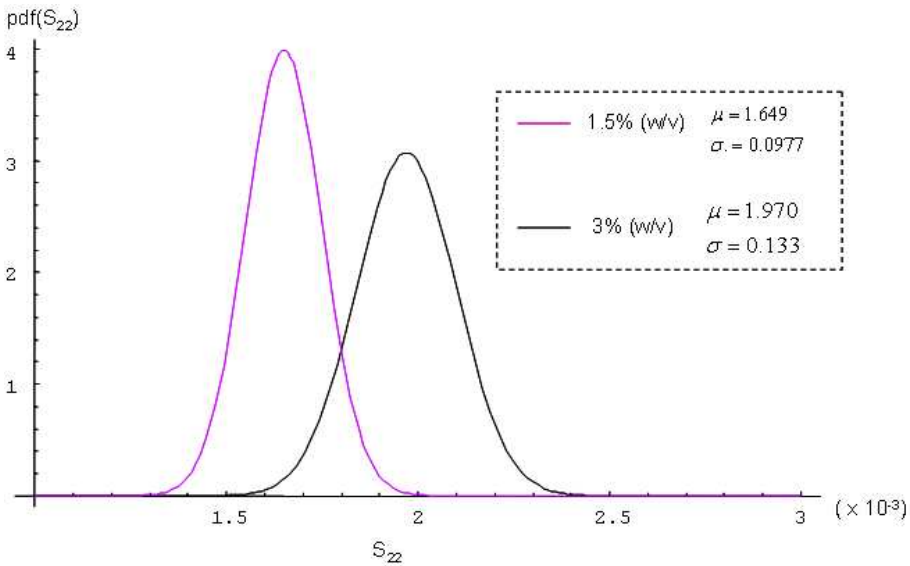


Figure 9. PDF plot of S_{22} (in MPa) with mean $\mu = 1.97 \times 10^{-3}$ and standard deviation $\sigma = 0.13 \times 10^{-3}$ for cells embedded in 1.5% w/v and 3% w/v alginate concentrations.

and the random cell distribution model. There is little variation between the two cases where the cell size is constant and is variable. We conclude, then, that cell size does not affect the results too much. Similar trend can be observed in the strain contour plots in the form of deformation. Hence, the cell distribution affects the analysis in a significant manner.

This work uses the multilevel finite element approach to analyze the cell's microenvironment when tissue scaffolds are subjected to macrolevel loads. Previous works of Breuls et al. [2002] and Guilak and Mow [2000] have also used the same approach to analyze the local deformations in the cell's surroundings. However, these studies do not provide an in-depth analysis in terms of the effects of the microlevel physical and geometrical heterogeneity on cell stress and deformation. This paper aims to address these factors and aids in estimating the degree of influence as well as the dominance among various parameters using a statistical approach. It must be noted that this paper does not attempt to explain how the computed stresses or deformations affect the function or the phenotype of the cell concerned. Our future studies will be aimed at validating this model by conducting biological experiments that can examine the function of the cells under different stress environments.

5. Conclusion

In this work we focus on quantifying the effects of microphysical and geometric heterogeneity on the endothelial cells encapsulated in alginate gel under load using the multilevel finite element approach. The macrolevel properties of cell encapsulated alginate discs have been characterized. The microlevel stresses and deformations that cells are subjected to under macrolevel loads are analyzed. Two different concentrations of alginate gel create different mechanical environments; the effects of material stiffness have been modeled to quantify cell deformation and stress distribution within the constructs. This is

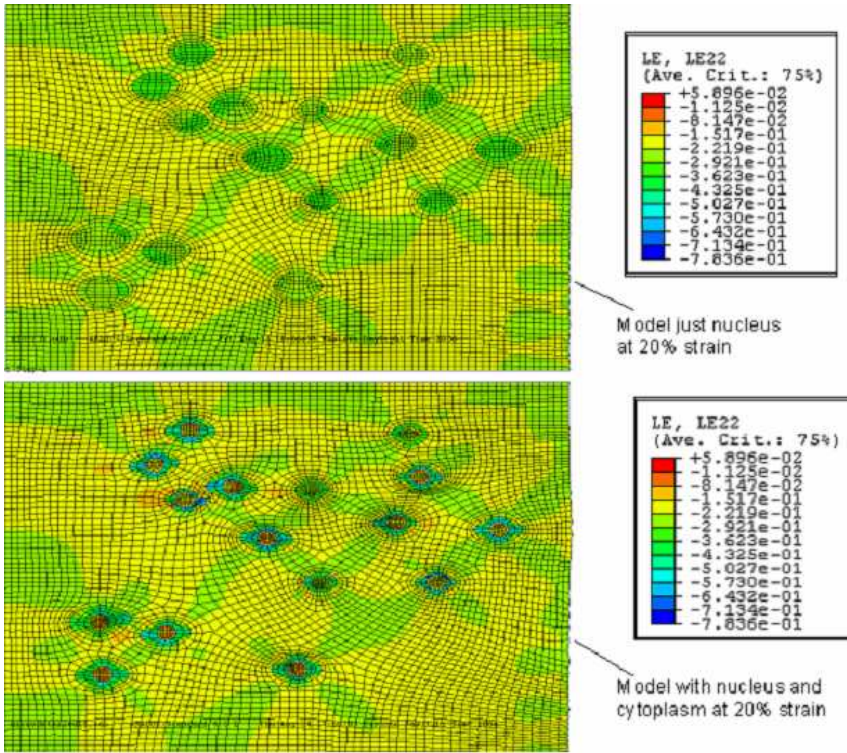


Figure 10. Logarithmic strain contour for analyzing effects of detailed microstructure.

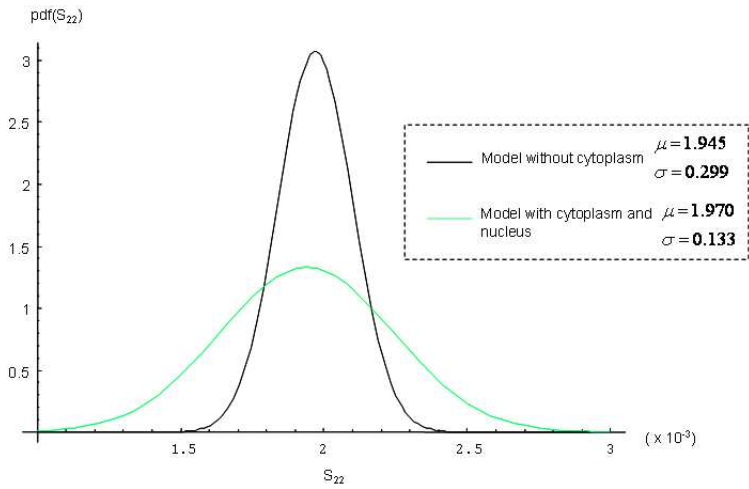


Figure 11. PDF plot of S_{22} (in MPa) with mean μ and standard deviation σ for analyzing effects of detailed microstructure.

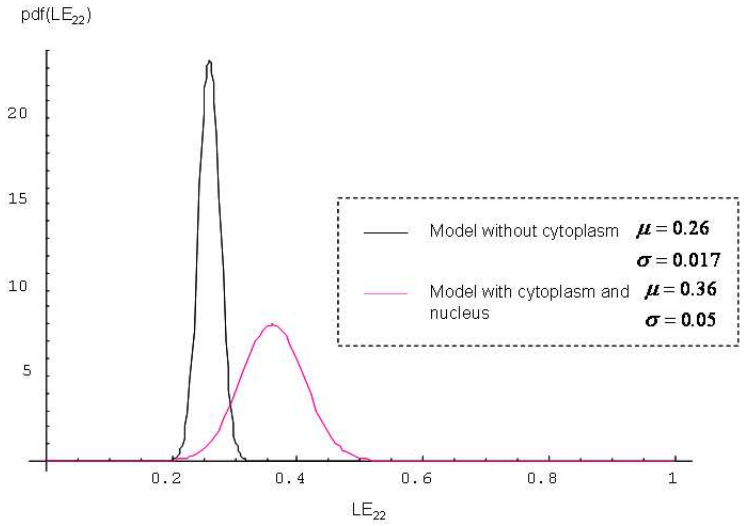


Figure 12. PDF plot of L_{22} with mean μ and standard deviation σ analyzing effects of detailed microstructure.

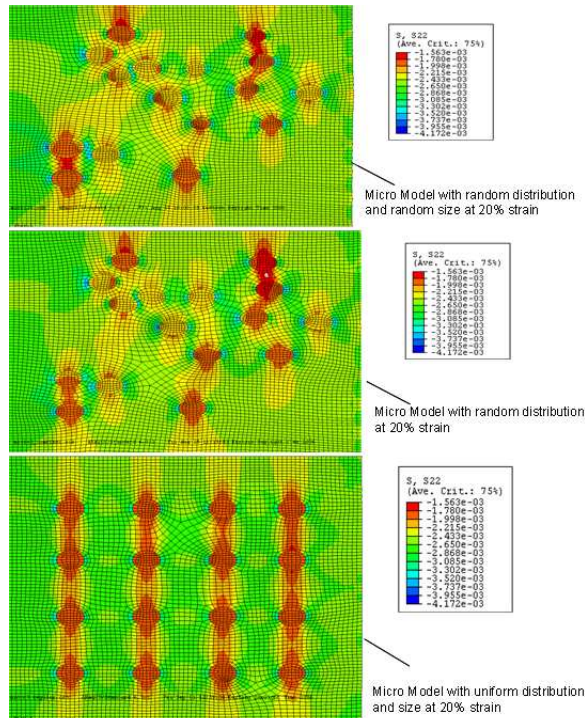


Figure 13. Stress (in MPa) contour analyzing effects of geometrical distribution in size and location of cells within the microstructure.

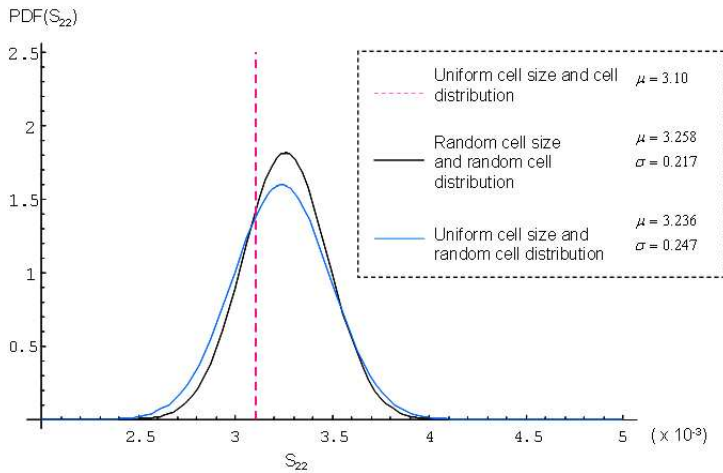


Figure 14. PDF plot of S_{22} (in MPa) with mean μ and standard deviation σ analyzing effects of geometrical distribution in size and location of cells within the microstructure.

critical in determining the right material parameters, specifically alginate concentration in this case, when fabricating three-dimensional scaffolds.

Secondly, the paper examined the modeling of the cell, with and without a distinction between the cytoplasm and nucleus in terms of material properties. From the single phase model, the cell can withstand higher stresses since the nucleus is much stiffer than the cytoplasm. However, in order to look into cell damage, it becomes imperative to identify the stresses at the cytoplasm which is much less stiff than the nucleus. Additional information obtained from the detailed model may be linked to membrane damage and cell injury.

Finally, this study also analyzes the effects of two geometrical parameters, cell size and cell distribution, on the local stress levels of the cell. This further allows us to understand the differences in terms of stresses and deformations at the cellular levels between the cases where the cells are isolated versus those where they are clustered. To some extent this helps in understanding cell-cell interactions as well. Additionally, studies aiming to understand how the computed stresses and/or deformations affect cell function or behavior will greatly strengthen the analysis. Future studies will include experimental validation of these models.

References

- [ABAQUS 2002] *ABAQUS user manual*, Version 6.3-1, Hibbit Karlsson Sorensen Inc., Providence, RI, 2002.
- [Bain 2001] B. J. Bain, *Blood cells: a practical guide*, 3rd ed., Blackwell Science, Oxford, 2001.
- [Bao and Suresh 2003] G. Bao and S. Suresh, “Cell and molecular mechanics of biological materials”, *Nat. Mater.* **2**:11 (2003), 715–725.
- [Boyce 2000] M. Boyce, “Constitutive models of rubber elasticity: a review”, *Rubber Chem. Technol.* **73**:3 (2000), 504–523.

- [Breuls et al. 2002] R. G. M. Breuls, B. G. Sengers, C. W. J. Oomens, C. V. C. Bouten, and F. P. T. Baaijens, “Predicting local cell deformations in engineered tissue constructs: a multilevel finite element approach”, *J. Biomech. Eng. (Trans. ASME)* **124**:2 (2002), 198–207.
- [Caille et al. 2002] N. Caille, O. Thoumine, Y. Tardy, and J. J. Meister, “Contribution of the nucleus to the mechanical properties of endothelial cells”, *J. Biomech.* **35**:2 (2002), 177–187.
- [Cines et al. 1998] D. B. Cines, E. S. Pollak, C. A. Buck, J. Loscalzo, G. A. Zimmerman, R. P. McEver, J. S. Pober, T. M. Wick, B. A. Konkle, B. S. Schwartz, E. S. Barnathan, K. R. McCrae, B. A. Hug, A. M. Schmidt, and D. M. Stern, “Endothelial cells in physiology and in the pathophysiology of vascular disorders”, *Blood* **91**:10 (1998), 3527–3561.
- [Dobrin 1978] P. B. Dobrin, “Mechanical properties of arterises”, *Physiol. Rev.* **58**:2 (1978), 397–460.
- [Drury et al. 2004] J. L. Drury, R. G. Dennis, and D. J. Mooney, “The tensile properties of alginate hydrogels”, *Biomaterials* **25**:16 (2004), 3187–3199.
- [Griffith and Swartz 2006] L. G. Griffith and M. A. Swartz, “Capturing complex 3D tissue physiology in vitro”, *Nat. Rev. Mol. Cell Biol.* **7**:3 (2006), 211–224.
- [Guilak and Mow 2000] F. Guilak and V. C. Mow, “The mechanical environment of the chondrocyte: a biphasic finite element model of cell-matrix interactions in articular cartilage”, *J. Biomech.* **33**:12 (2000), 1663–1673.
- [Haider et al. 2006] M. A. Haider, R. C. Schugart, L. A. Setton, and F. A. Guilak, “A mechano-chemical model for the passive swelling response of an isolated chondron under osmotic loading”, *Biomech. Modeling Mechanobiol.* **5**:2-3 (2006), 160–171.
- [Ingber 1997] D. E. Ingber, “Tensegrity: the architectural basis of cellular mechanotransduction”, *Annu. Rev. Physiol.* **59** (1997), 575–599.
- [Khalil 2006] S. Khalil, *Deposition and structural formation of 3D alginate tissue scaffolds*, Ph.D. thesis, Drexel University, Philadelphia, PA, 2006, Available at <http://hdl.handle.net/1860/664>.
- [Khalil et al. 2005] S. Khalil, J. Nam, and W. Sun, “Multi-nozzle deposition for construction of 3D biopolymer tissue scaffolds”, *Rapid Prototyping J.* **11**:1 (2005), 9–17.
- [Kouznetsova et al. 2001] V. Kouznetsova, W. A. M. Brekelmans, and F. P. T. Baaijens, “An approach to micro-macro modeling of heterogeneous materials”, *Comput. Mech.* **27**:1 (2001), 37–48.
- [Pelham and Wang 1997] J. R. Pelham and Y. Wang, “Cell locomotion and focal adhesions are regulated by substrate flexibility”, *P. Natl. Acad. Sci. USA* **94**:25 (1997), 13661–13665.
- [Quintanilla and Torquato 1997] J. Quintanilla and S. Torquato, “Local volume fraction fluctuations in random media”, *J. Chem. Phys.* **106**:7 (1997), 2741–2751.
- [Smit et al. 1998] R. J. M. Smit, W. A. M. Brekelmans, and H. E. H. Meijer, “Prediction of the mechanical behavior of nonlinear heterogeneous systems by multi-level finite element modeling”, *Comput. Methods Appl. Mech. Eng.* **155**:1–2 (1998), 181–192.
- [Smit et al. 1999] R. J. M. Smit, W. A. M. Brekelmans, and H. E. H. Meijer, “Prediction of the large-strain mechanical response of heterogeneous polymer systems: local and global deformation behaviour of a representative volume element of voided polycarbonate”, *J. Mech. Phys. Solids* **47**:2 (1999), 201–221.
- [Torquato 1998] S. Torquato, “Morphology and effective properties of disordered heterogeneous media”, *Int. J. Solids Struct.* **35**:19 (1998), 2385–2406.
- [Wang and Yan 2005] A. S. D. Wang and K. C. Yan, “On modeling matrix failures in composites”, *Compos. A Appl. Sci. Manuf.* **36**:10 (2005), 1335–1346.
- [Wedding et al. 2002] K. L. Wedding, M. T. Draney, R. J. Herfkens, C. K. Zarins, C. A. Taylor, and N. J. Pelc, “Measurement of vessel wall strain using cine phase contrast MRI”, *J. Magn. Reson. Imaging* **15**:4 (2002), 418–428.
- [Wille et al. 2004] J. J. Wille, C. M. Ambrosi, and F. C. P. Yin, “Comparison of the effects of cyclic stretching and compression on endothelial cell morphological responses”, *J. Biomech. Eng. (Trans. ASME)* **126**:5 (2004), 545–551.

Received 20 Feb 2007. Accepted 24 Feb 2007.

KALYANI NAIR: kn43@drexel.edu

Department of Mechanical Engineering and Mechanics, Drexel University, 32nd and Chestnut Street, Philadelphia, PA 19104, United States

KAREN CHANG YAN: yan@tcnj.edu

Department of Mechanical Engineering, The College of New Jersey, Ewing, NJ 08628, United States

WEI SUN: sunwei@drexel.edu

Department of Mechanical Engineering and Mechanics, Drexel University, 32nd and Chestnut Street, Philadelphia, PA 19104, United States

